threshold for clumped SNPs = 0.01, r^2 = 0.25, physical distance = 1 Mb; Extended Data Fig. 6b). Regions with the strongest genetic similarity were grouped together based on the strength of their pairwise correlations. The results were represented visually using hierarchical clustering with default settings from the gplots package (version 2.12.1) in R.

Gene annotation, gene-based test statistics and pathway analysis were performed using the KGG2.5 software package[42] (Supplementary Table 7 and Extended Data Fig. 7). Linkage disequilibrium was calculated based on RSID numbers using the 1000 Genomes Project European samples as a reference (http://enigma.ini.usc.edu/protocols/genetics-protocols/). For the annotation, SNPs were considered 'within' a gene if they fell within 5 kb of the 3′/5′ untranslated regions based on human genome (hg19) coordinates. Gene-based tests were performed using the GATES test[42] without weighting P values by predicted functional relevance. Pathway analysis was performed using the hybrid set-based test (HYST) of association[43]. For all gene-based tests and pathway analyses, results were considered significant if they exceeded a Bonferroni correction threshold accounting for the number of pathways and traits tested such that $P_{thresh} = 0.05/(671 \text{ pathways} \times 7 \text{ independent traits}) = 1.06 \times 10^{-5}$.

Expression quantitative loci were examined in two independent data sets: the NABEC (GSE36192)[24] and UKBEC (GSE46706)[44,45]. Detailed processing and exclusion criteria for both data sets are described elsewhere[24,45]. In brief, the UKBEC consists of 134 neuropathologically normal donors from the MRC Sudden Death Brain Bank in Edinburgh and Sun Health Research Institute; expression was profiled on the Affymetrix Exon 1.0 ST array. The NABEC is comprised of 304 neurologically normal donors from the National Institute of Ageing and expression profiled on the Illumina HT12v3 array. The expression values were corrected for gender and batch effects and probes that contained polymorphisms (seen >1% in European 1000G) were excluded from analyses[44]. Blood expression quantitative trait loci (eQTL) data were queried using the Blood eQTL Browser (http://genenetwork.nl/bloodeqtlbrowser/)[26]. Brain expression over the lifespan was measured from a spatio-temporal atlas of human gene expression and graphed using custom R scripts (GSE25219; details given in[13]).

Fine-grained three-dimensional surface mappings of the putamen were generated using a medial surface modelling method[46,47] in 1,541 healthy subjects from the IMAGEN study[48] (Fig. 2c and Extended Data Fig. 10a, b). Putamen volume segmentations from either FSL (Fig. 2c and Extended Data Fig. 10a) or FreeSurfer (Extended Data Fig. 10b) were first converted to three-dimensional meshes and then co-registered to an average template for statistical analysis. The medial core distance was used as a measure of shape and was calculated as the distance from each point on the surface to the centre of the putamen. At each point along the surface of the putamen, an association test was performed using multiple linear regression in which the medial core distance at a given point on the surface was the outcome measure and the additive dosage value of the top SNP was the predictor of interest while including the same covariates that were used for volume including age, sex, age^2, 4 MDS, ICV and site.

In Extended Data Fig. 3, all tracks were taken from the UCSC Genome Browser Human hg19 assembly. SNPs (top 5%) shows the top 5% associated SNPs within the locus and are coloured by their correlation to the top SNP. Genes shows the gene models from GENCODE version 19. Conservation was defined at each base through the phyloP algorithm which assigns scores as $-\log_{10} P$ values under a null hypothesis of neutral evolution calculated from pre-computed genomic alignment of 100 vertebrate species[49]. Conserved sites are assigned positive scores, while faster-than-neutral evolving sites are given negative scores. TFBS conserved shows computationally predicted transcription factor binding sites using the Transfac Matrix Database (v.7.0) found in human, mouse and rat. Brain histone (1.3 year) and brain histone (68 year) show maps of histone trimethylation at histone H3 Lys 4 (H3K4me3), an epigenetic mark for transcriptional activation, measured by ChIP-seq. These measurements were made in neuronal nuclei (NeuN+) collected from prefrontal cortex of post-mortem human brain[50]. CpG methylation was generated using methylated DNA immunoprecipitation and sequencing from postmortem human frontal cortex of a 57-year-old male[51]. DNaseI hypersens displays DNaseI hypersensitivity, evidence of open chromatin, which was evaluated in postmortem human frontal cerebrum from three donors (age 22–35), through the ENCODE consortium[52]. Finally, hES Chrom State gives the predicted chromatin states based on computational integration of ChIP-seq data for nine chromatin marks in H1 human embryonic stem cell lines derived in the ENCODE consortium[53].

31. Patenaude, B., Smith, S. M., Kennedy, D. N. & Jenkinson, M. A Bayesian model of shape and appearance for subcortical brain segmentation. *Neuroimage* **56,** 907–922 (2011).
32. Fischl, B. *et al.* Whole brain segmentation: automated labeling of neuroanatomical structures in the human brain. *Neuron* **33,** 341–355 (2002).
33. Morey, R. A. *et al.* Scan-rescan reliability of subcortical brain volumes derived from automated segmentation. *Hum. Brain Mapp.* **31,** 1751–1762 (2010).
34. Li, Y., Willer, C. J., Ding, J., Scheet, P. & Abecasis, G. R. MaCH: using sequence and genotype data to estimate haplotypes and unobserved genotypes. *Genet. Epidemiol.* **34,** 816–834 (2010).
35. Howie, B., Fuchsberger, C., Stephens, M., Marchini, J. & Abecasis, G. R. Fast and accurate genotype imputation in genome-wide association studies through pre-phasing. *Nature Genet.* **44,** 955–959 (2012).
36. Abecasis, G. R., Cherny, S. S., Cookson, W. O. & Cardon, L. R. Merlin-rapid analysis of dense genetic maps using sparse gene flow trees. *Nature Genet.* **30,** 97–101 (2002).
37. Willer, C. J., Li, Y. & Abecasis, G. R. METAL: fast and efficient meta-analysis of genomewide association scans. *Bioinformatics* **26,** 2190–2191 (2010).
38. Nyholt, D. R. A simple correction for multiple testing for single-nucleotide polymorphisms in linkage disequilibrium with each other. *Am. J. Hum. Genet.* **74,** 765–769 (2004).
39. Boker, S. *et al.* OpenMx: an open source extended structural equation modeling framework. *Psychometrika* **76,** 306–317 (2011).
40. Walters, R., Bartels, M. & Lubke, G. Estimating variance explained by all variants in meta-analysis with heterogeneity. *Behav. Genet.* **43,** 543 (2013).
41. So, H. C., Li, M. & Sham, P. C. Uncovering the total heritability explained by all true susceptibility variants in a genome-wide association study. *Genet. Epidemiol.* **35,** 447–456 (2011).
42. Li, M. X., Gui, H. S., Kwan, J. S. & Sham, P. C. GATES: a rapid and powerful gene-based association test using extended Simes procedure. *Am. J. Hum. Genet.* **88,** 283–293 (2011).
43. Li, M. X., Kwan, J. S. & Sham, P. C. HYST: a hybrid set-based test for genome-wide association studies, with application to protein-protein interaction-based association analysis. *Am. J. Hum. Genet.* **91,** 478–488 (2012).
44. Ramasamy, A. *et al.* Resolving the polymorphism-in-probe problem is critical for correct interpretation of expression QTL studies. *Nucleic Acids Res.* **41,** e88 (2013).
45. Trabzuni, D. *et al.* Quality control parameters on a large dataset of regionally dissected human control brains for whole genome expression studies. *J. Neurochem.* **119,** 275–282 (2011).
46. Gutman, B. A. *et al.* Maximizing power to track Alzheimer's disease and MCI progression by LDA-based weighting of longitudinal ventricular surface features. *Neuroimage* **70,** 386–401 (2013).
47. Gutman, B. A., Wang, Y. L., Rajagopalan, P., Toga, A. W. & Thompson, P. M. Shape matching with medial curves and 1-d group-wise registration. In *2012 9th IEEE International Symposium on Biomedical Imaging (ISBI)*, 716–719 (2012).
48. Schumann, G. *et al.* The IMAGEN study: reinforcement-related behaviour in normal brain function and psychopathology. *Mol. Psychiatry* **15,** 1128–1139 (2010).
49. Pollard, K. S., Hubisz, M. J., Rosenbloom, K. R. & Siepel, A. Detection of nonneutral substitution rates on mammalian phylogenies. *Genome Res.* **20,** 110–121 (2010).
50. Cheung, I. *et al.* Developmental regulation and individual differences of neuronal H3K4me3 epigenomes in the prefrontal cortex. *Proc. Natl Acad. Sci. USA* **107,** 8824–8829 (2010).
51. Maunakea, A. K. *et al.* Conserved role of intragenic DNA methylation in regulating alternative promoters. *Nature* **466,** 253–257 (2010).
52. Boyle, A. P. *et al.* High-resolution mapping and characterization of open chromatin across the genome. *Cell* **132,** 311–322 (2008).
53. Ernst, J. *et al.* Mapping and analysis of chromatin state dynamics in nine human cell types. *Nature* **473,** 43–49 (2011).
54. Devlin, B. & Roeder, K. Genomic control for association studies. *Biometrics* **55,** 997–1004 (1999).
55. Hager, R., Lu, L., Rosen, G. D. & Williams, R. W. Genetic architecture supports mosaic brain evolution and independent brain-body size regulation. *Nat. Commun.* **3,** 1079 (2012).
56. Schmucker, D. & Chen, B. Dscam and DSCAM: complex genes in simple animals, complex animals yet simple genes. *Genes Dev.* **23,** 147–156 (2009).
57. Brunet, A., Datta, S. R. & Greenberg, M. E. Transcription-dependent and -independent control of neuronal survival by the PI3K-Akt signaling pathway. *Curr. Opin. Neurobiol.* **11,** 297–305 (2001).

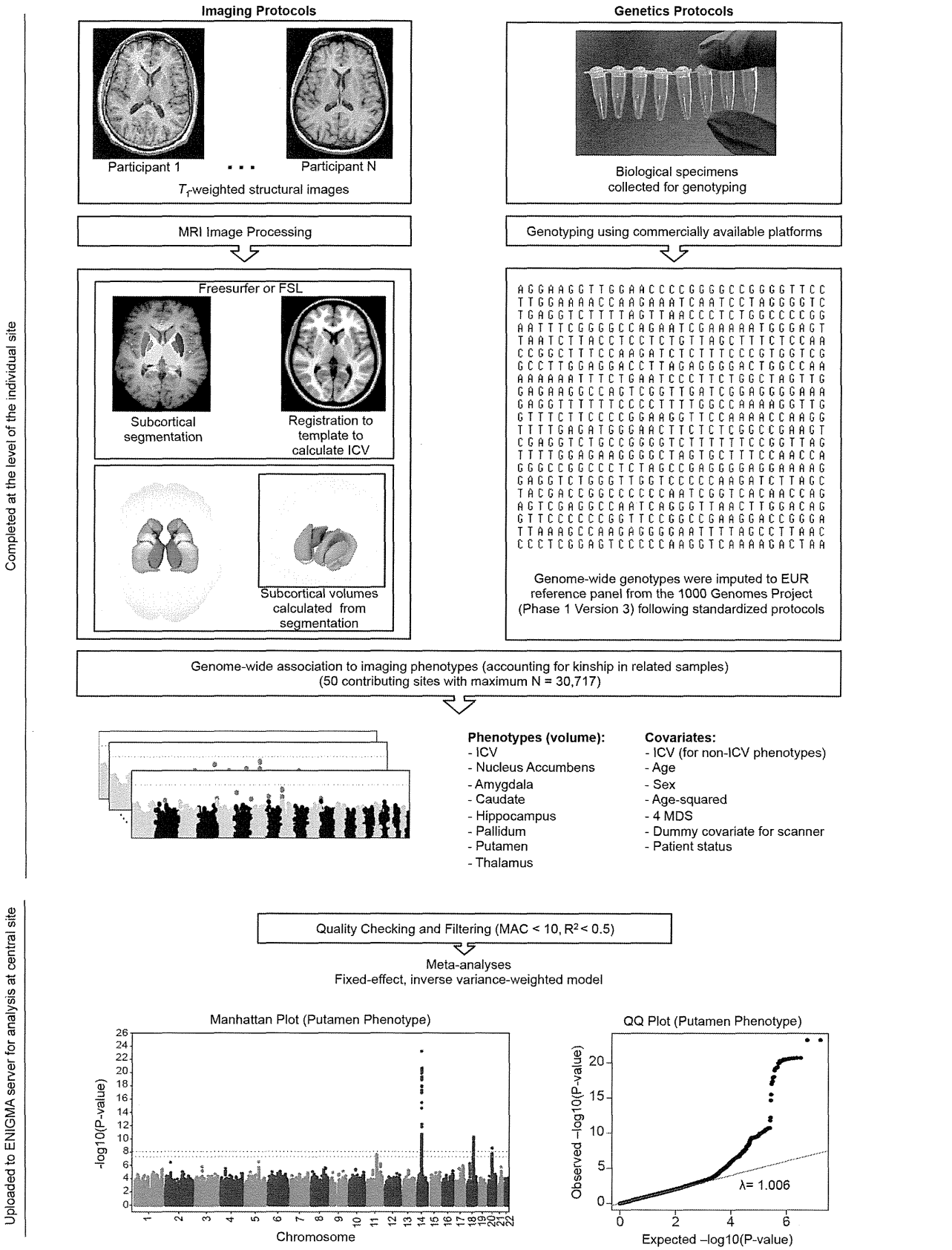

Extended Data Figure 1 | Outline of the genome-wide association meta-analysis. Structural T_1-weighted brain MRI and biological specimens for DNA extraction were acquired from each individual at each site. Imaging protocols were distributed to and completed by each site for standardized automated segmentation of brain structures and calculation of the ICV. Volumetric phenotypes were calculated from the segmentations. Genome-wide genotyping was completed at each site using commercially available chips. Standard imputation protocols to the 1000 Genomes reference panel (phase 1, version 3) were also distributed and completed at each site. Each site completed genome-wide association for each of the eight volumetric brain phenotypes with the listed covariates. Statistical results from GWAS files were uploaded to a central site for quality checking and fixed effects meta-analysis.

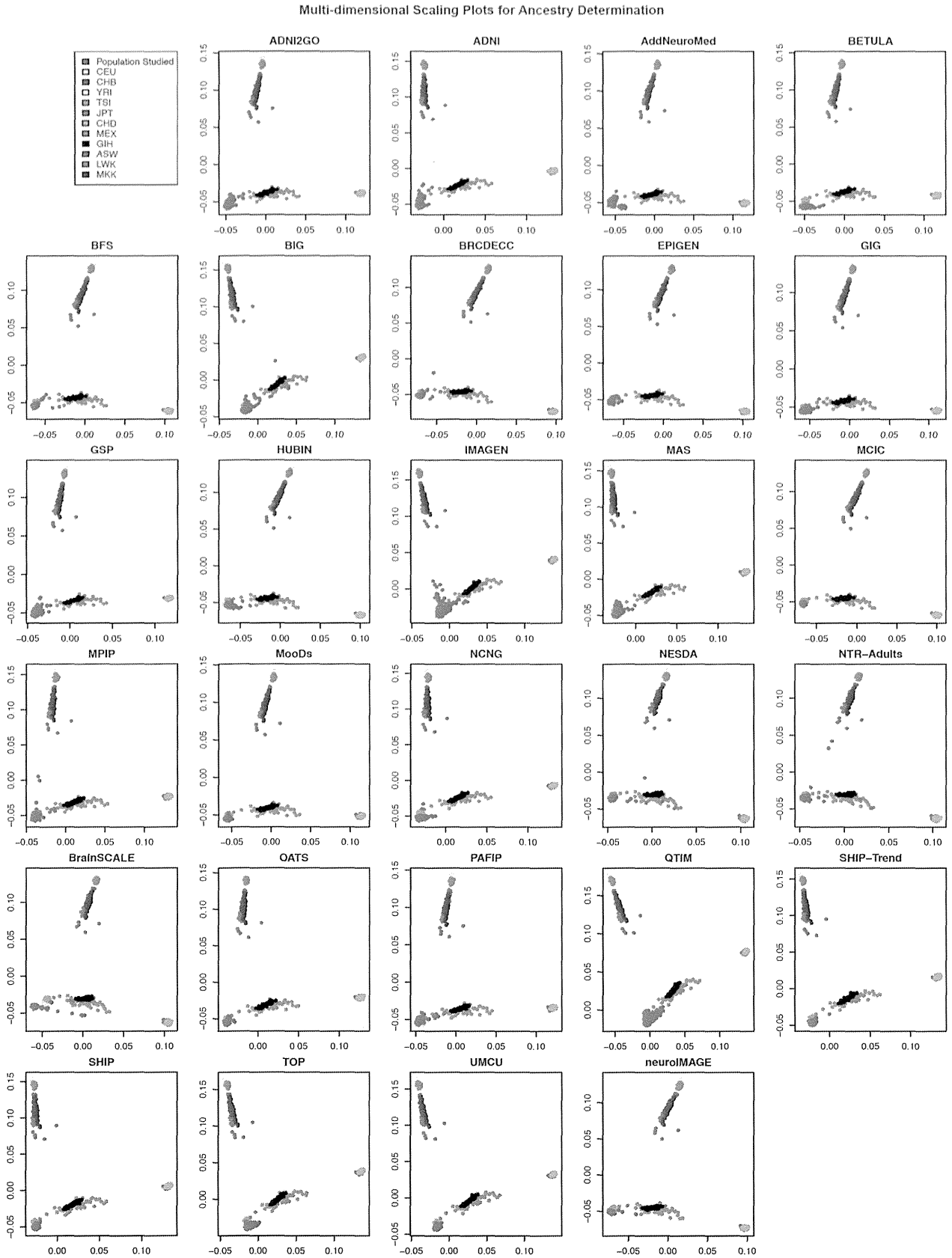

Extended Data Figure 2 | Ancestry inference via multi-dimensional scaling plots. Multi-dimensional scaling (MDS) plots of the discovery cohorts to HapMap III reference panels of known ancestry are displayed. Ancestry is generally homogeneous within each group. In all discovery samples any individuals with non-European ancestry were excluded before association. The axes have been flipped to the same orientation for each sample for ease of comparison. ASW, African ancestry in southwest USA; CEU, Utah residents with northern and western European ancestry from the CEPH collection; CHD, Chinese in metropolitan Denver, Colorado; GIH, Gujarati Indians in Houston, Texas; LWK, Luhya in Webuye, Kenya; MEX, Mexican ancestry in Los Angeles, California; MKK, Maasai in Kinyawa, Kenya; TSI, Tuscans in Italy; YRI, Yoruba in Ibadan, Nigeria.

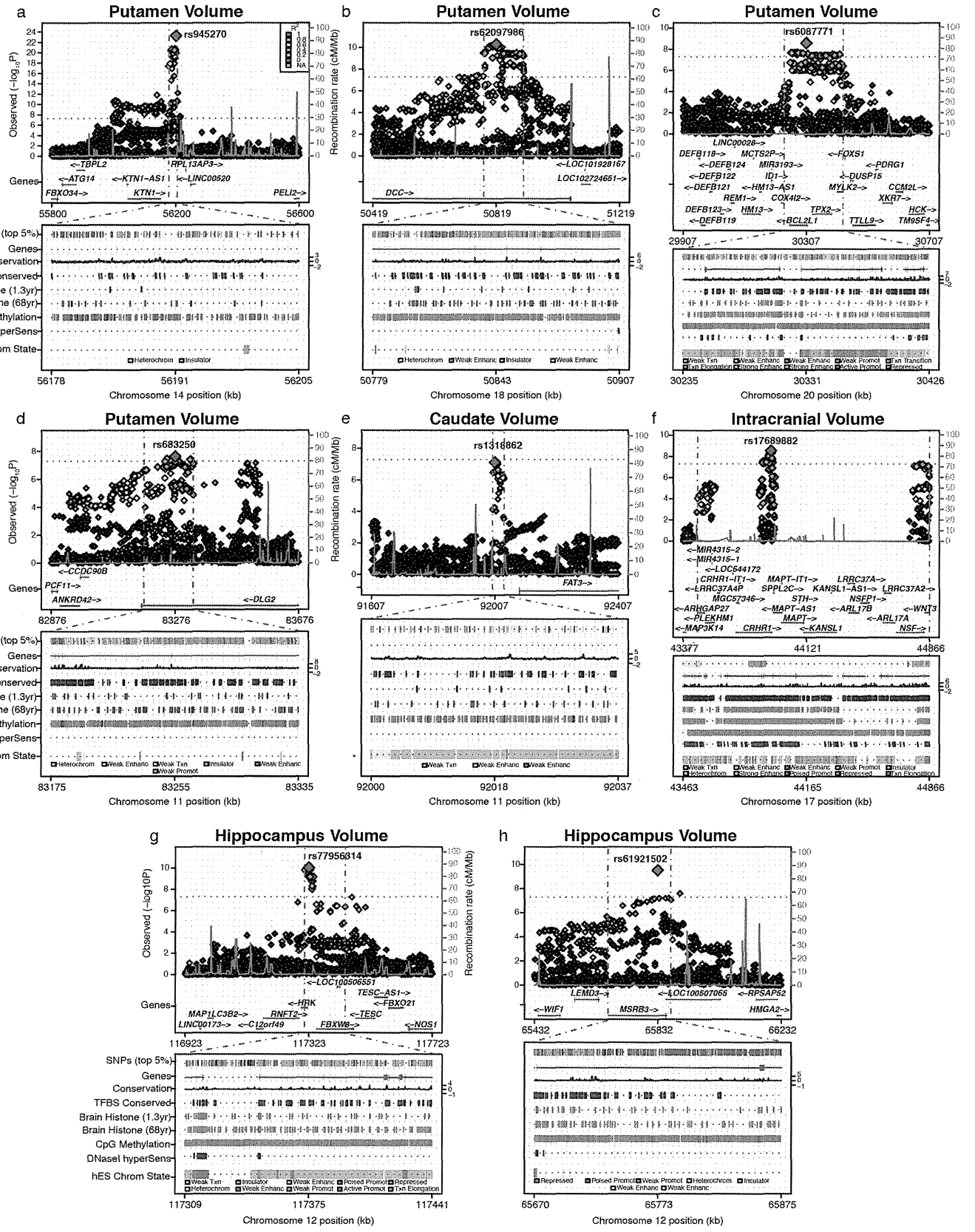

Extended Data Figure 3 | Genomic function is annotated near novel genome-wide significant loci. a–h, For each panel, zoomed-in Manhattan plots (±400 kb from top SNP) are shown with gene models below (GENCODE version 19). Plots below are zoomed to highlight the genomic region that probably contains the causal variant(s) ($r^2 > 0.8$ from the top SNP). Genomic annotations from the UCSC browser and ENCODE are displayed to indicate potential functionality (see Methods for detailed track information). SNP coverage is low in **f** owing to a common genetic inversion in the region. Each plot was made using the LocusTrack software (http://gump.qimr.edu.au/general/gabrieC/LocusTrack/).

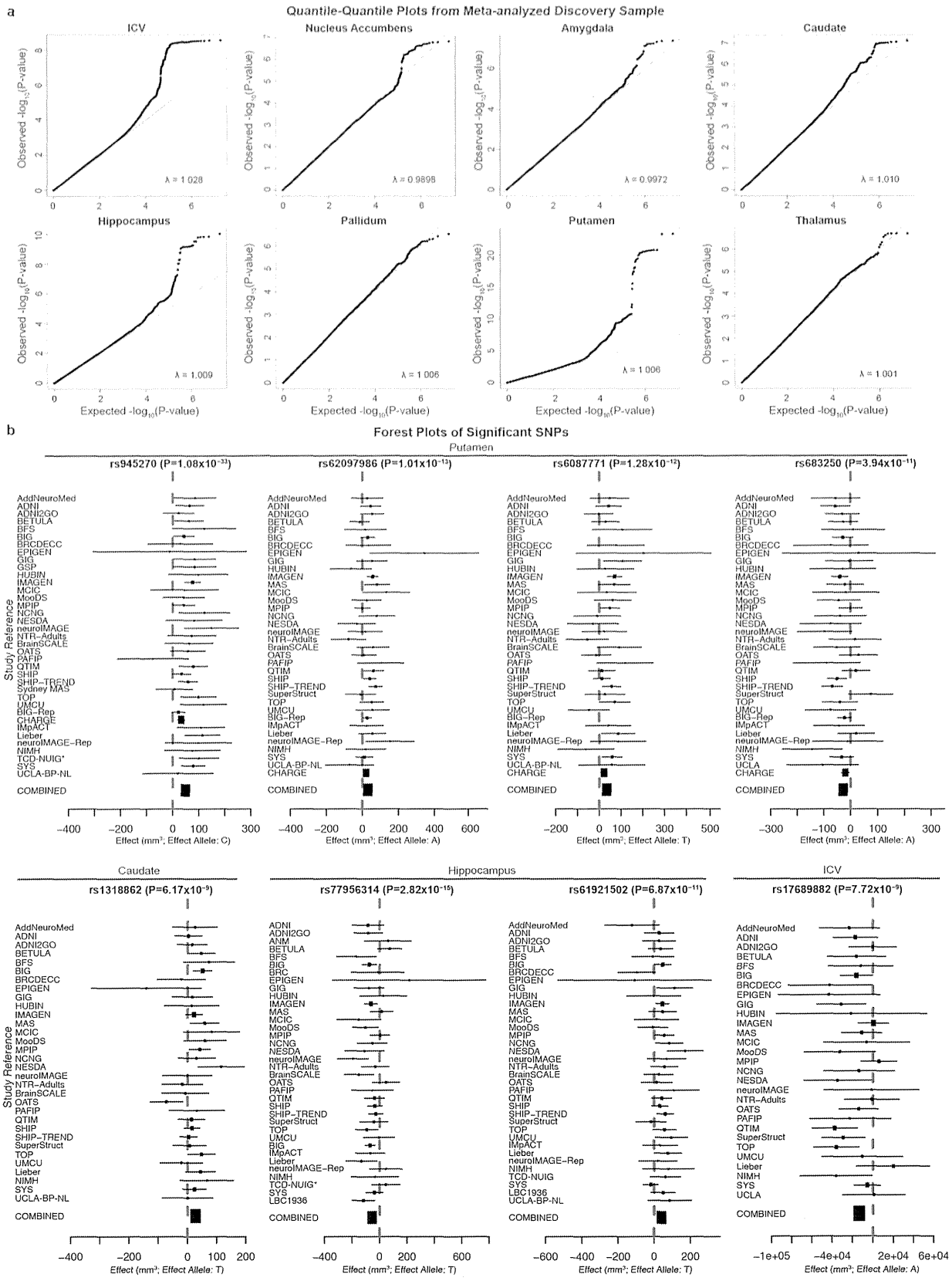

Extended Data Figure 4 | Quantile–quantile and forest plots from meta-analysis of discovery cohorts. **a**, Quantile–quantile plots show that the observed *P* values only deviate from the expected null distribution at the most significant values, indicating that population stratification or cryptic relatedness are not unduly inflating the results. This is quantified through the genomic control parameter (λ; which evaluates whether the median test statistic deviates from expected)[54]. λ values near 1 indicate that the median test statistic is similar to those derived from a null distribution. Corresponding meta-analysis Manhattan plots can be found in Fig. 1. **b**, Forest plots show the effect at each of the contributing sites to the meta-analysis. The size of the dot is proportional to the sample size, the effect is shown by the position on the *x* axis, and the standard error is shown by the line. Sites with an asterisk indicate the genotyping of a proxy SNP (in perfect linkage disequilibrium calculated from 1000 Genomes) for replication.

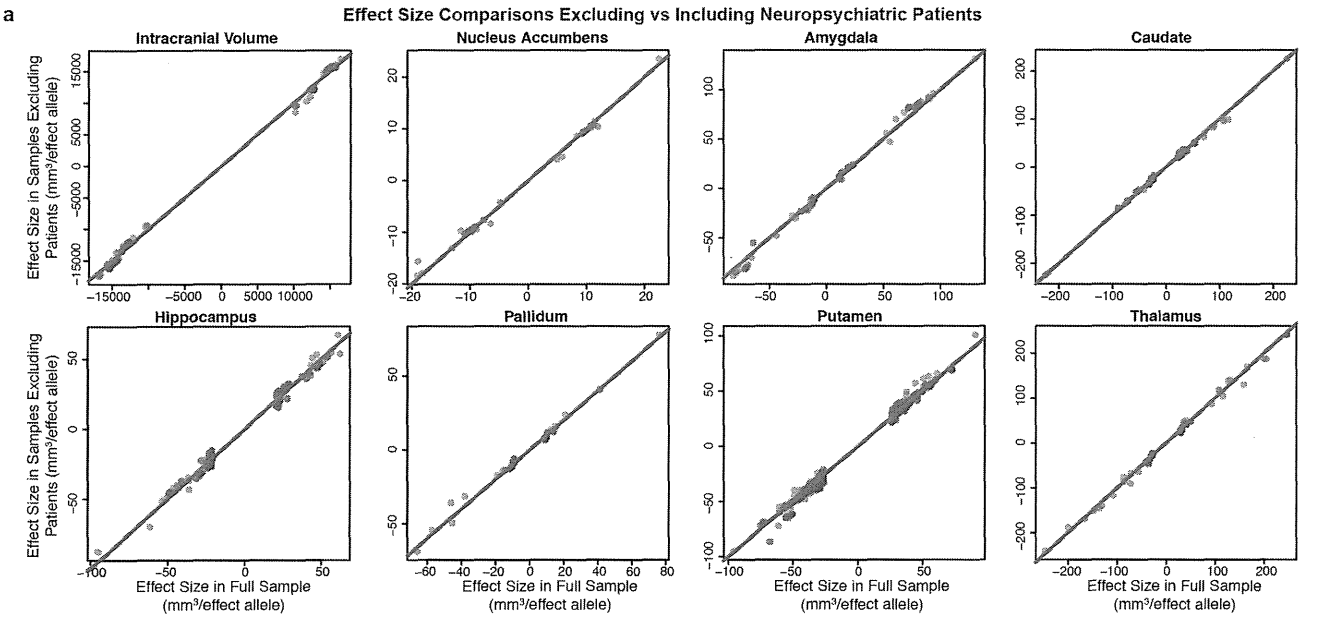

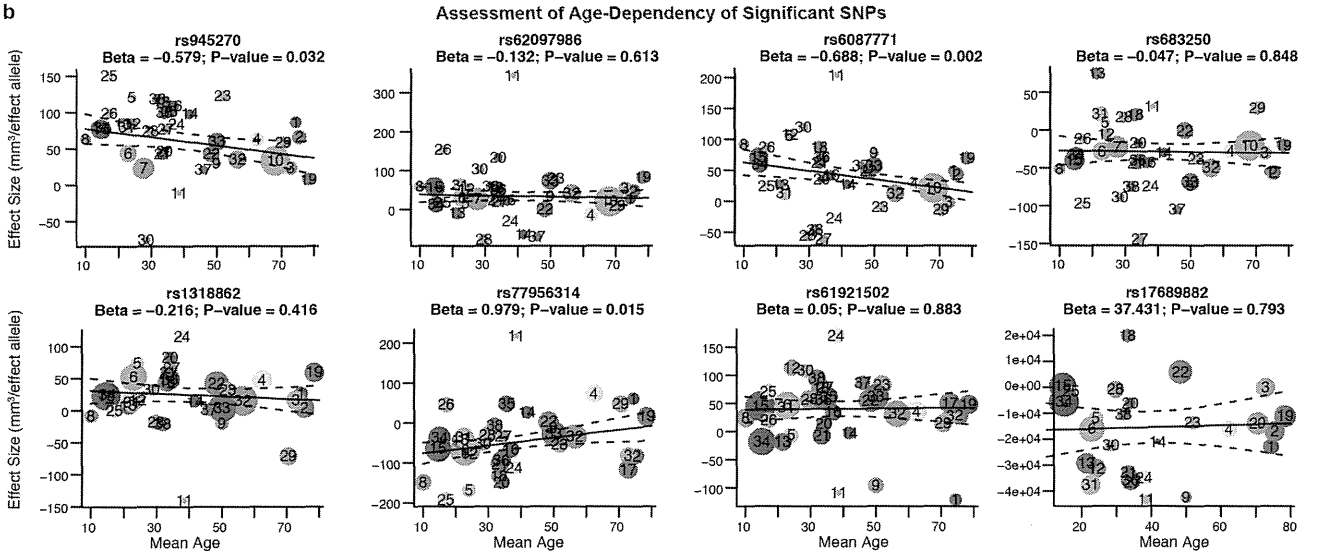

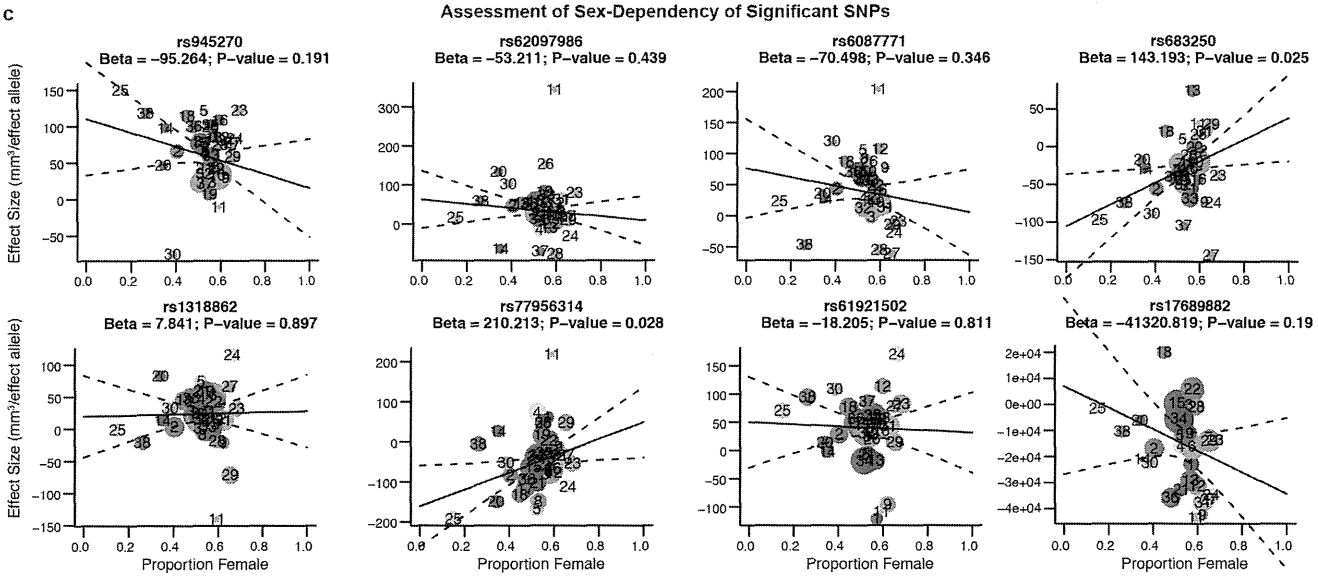

Extended Data Figure 5 | Influence of patients with neuropsychiatric disease, age and gender on association results. **a**, Scatterplot of effect sizes including and excluding patients with neuropsychiatric disorders for nominally significant SNPs. For each of the eight volumetric phenotypes, SNPs with $P < 1 \times 10^{-5}$ in the full discovery set meta-analysis were also evaluated excluding the patients. The beta values from regression, a measure of effect size, are plotted (blue dots) along with a line of equivalence between the two conditions (red line). The correlation between effect sizes with and without patients was very high ($r > 0.99$), showing that the SNPs with significant effects on brain structure are unlikely to be driven by the diseased individuals. **b**, Meta-regression comparison of effect size with mean age at each site. Each site has a corresponding number and coloured dot in each graph. The size of each dot is based on the standard error such that bigger sites with more definitive estimates have larger dots (and more influence on the meta-regression). The age range of participants covered most of the lifespan (9–97 years), but only one of these eight loci showed a significant relationship with the mean age of each cohort (rs608771 affecting putamen volume). **c**, Meta-regression comparison of effect size with the proportion of females at each site. No loci showed evidence of moderation by the proportion of females in a given sample. However, the proportion of females at each site has a very restricted range, so results should be interpreted with caution. Plotted information follows the same convention as described in **b**. The sites are numbered in the following order: (1) AddNeuroMed, (2) ADNI, (3) ADNI2GO, (4) BETULA, (5) BFS, (6) BIG, (7) BIG-Rep, (8) BrainSCALE, (9) BRCDECC, (10) CHARGE, (11) EPIGEN, (12) GIG, (13) GSP, (14) HUBIN, (15) IMAGEN, (16) IMpACT, (17) LBC1936, (18) Lieber, (19) MAS, (20) MCIC, (21) MooDS, (22) MPIP, (23) NCNG, (24) NESDA, (25) neuroIMAGE, (26) neuroIMAGE-Rep, (27) NIMH, (28) NTR-Adults, (29) OATS, (30) PAFIP, (31) QTIM, (32) SHIP, (33) SHIP-TREND, (34) SYS, (35) TCD-NUIG, (36) TOP, (37) UCLA-BP-NL and (38) UMCU.

a

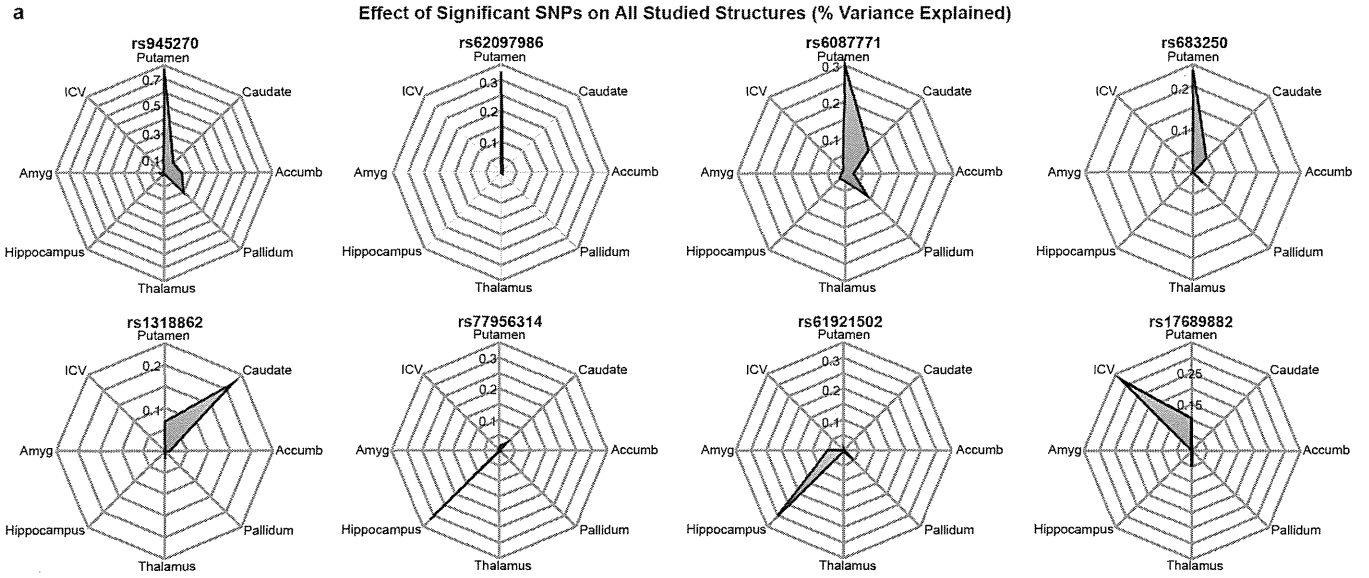

b

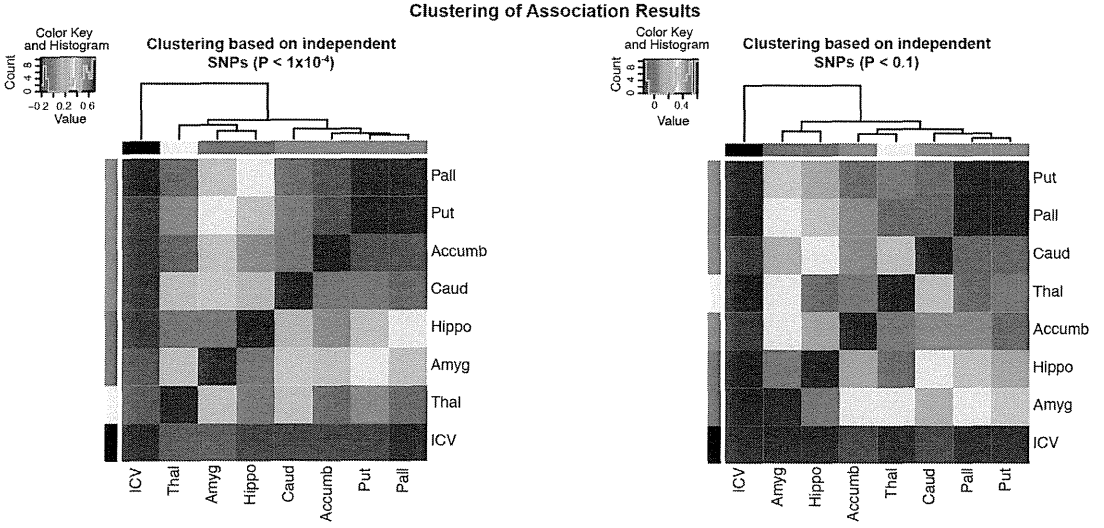

c

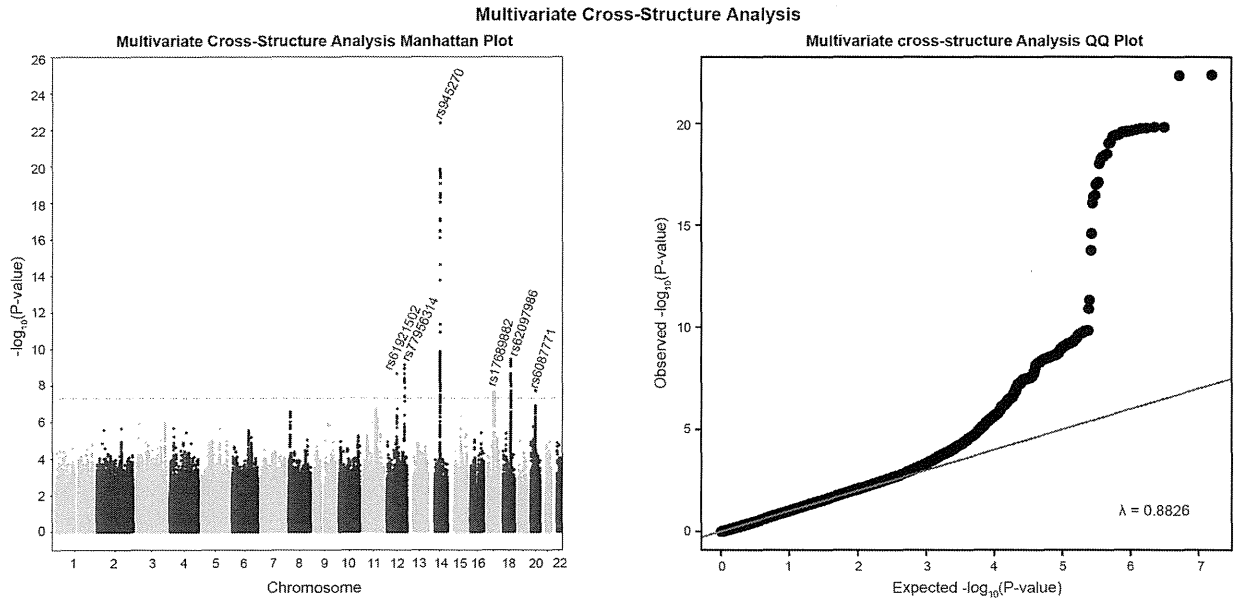

Extended Data Figure 6 | Cross-structure analyses. **a**, Radial plots of effect sizes from the discovery sample for all genome-wide significant SNPs identified in this study. Plots indicate the effect of each genetic variant, quantified as percentage variance explained, on the eight volumetric phenotypes studied. As expected, the SNPs identified with influence on a phenotype show the highest effect size for that phenotype: putamen volume (rs945270, rs62097986, rs608771 and rs683250), hippocampal volume (rs77956314 and rs61921502), caudate volume (rs1318862) and ICV (rs17689882). In general much smaller effects are observed on other structures. **b**, Correlation heat map of GWAS test statistics (*t*-values) and hierarchical clustering[55]. Independent SNPs were chosen within an linkage disequilibrium block based on the highest association in the multivariate cross-structure analysis described in Extended Data Fig. 6c. Two heat maps are shown taking only independent SNPs with either $P < 1 \times 10^{-4}$ (left) or $P < 0.01$ (right) in the multivariate cross-structure analysis. Different structures are labelled in developmentally similar regions by the colour bar on the top and side of the heat map including basal ganglia (putamen, pallidum, caudate and accumbens; blue), amygdalo–hippocampal complex (hippocampus and amygdala; red), thalamus (turquoise) and ICV (black). Hierarchical clustering showed that developmentally similar regions have mostly similar genetic influences across the entire genome. The low correlation with the ICV is owing to it being used as a covariate in the subcortical structure GWAS associations. **c**, A multivariate cross-structure analysis of all volumetric brain traits. A Manhattan plot (left) and corresponding quantile–quantile plot (right) of multivariate GWAS analysis of all traits (volumes of the accumbens, amygdala, caudate, hippocampus, pallidum, putamen, thalamus, and ICV) in the discovery data set using the TATES method[9] is shown. Multivariate cross-structure analysis confirmed the univariate analyses (see Table 1), but did not reveal any additional loci achieving cross-structure levels of significance.

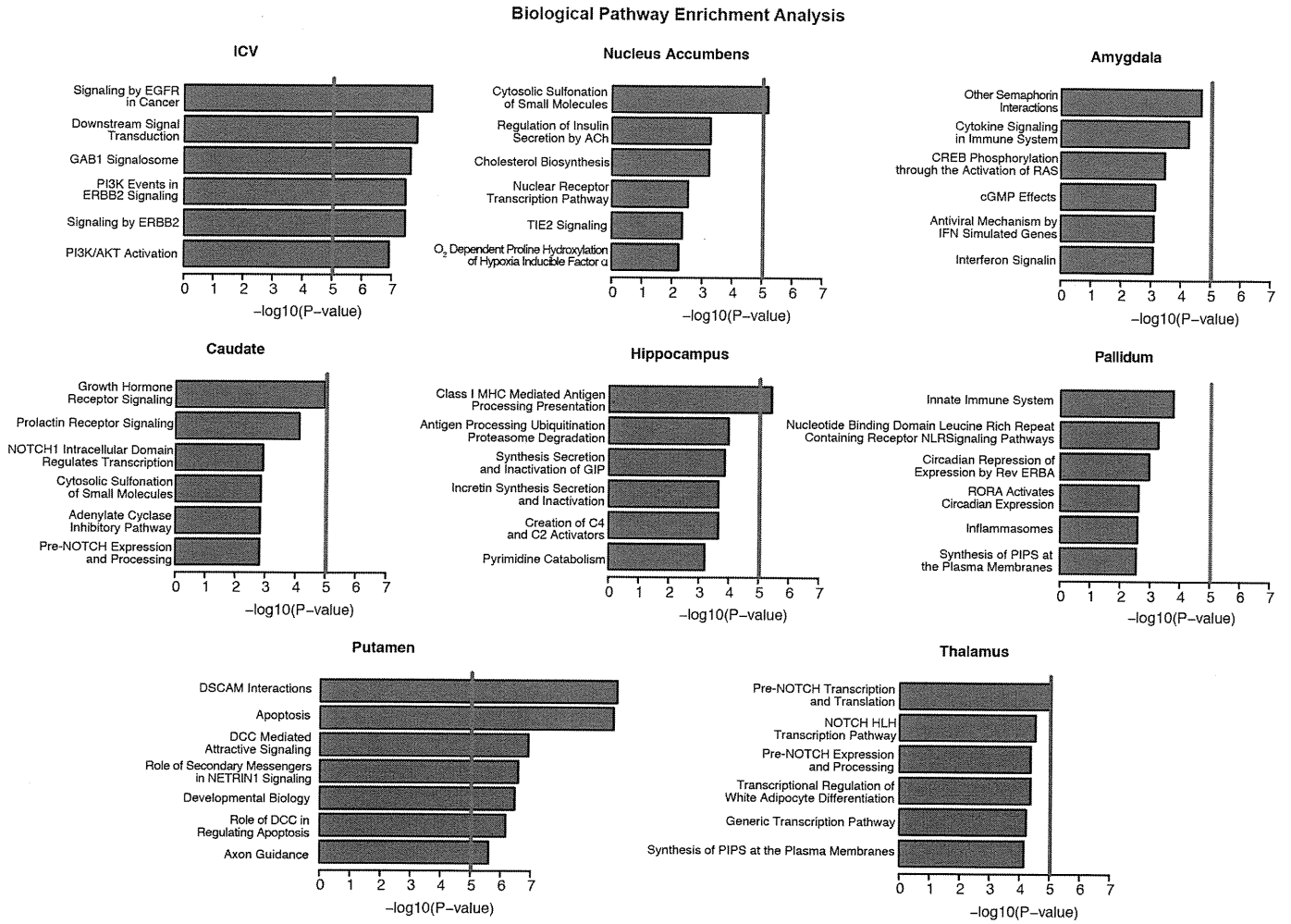

Extended Data Figure 7 | Pathway analysis of GWAS results for each brain structure. A pathway analysis was performed on each brain volume GWAS using KGG[42] to conduct gene-based tests and the Reactome database for pathway definition[43]. Pathway-wide significance was calculated using a Bonferroni correction threshold accounting for the number of pathways and traits tested such that $P_{thresh} = 0.05/(671 \text{ pathways} \times 7 \text{ independent traits}) = 1.06 \times 10^{-5}$ and is shown here as a red line. The number of independent traits was calculated by accounting for the non-independence of each of the eight traits examined (described in the Methods). Variants that influence the putamen were clustered near genes known to be involved in DSCAM interactions, neuronal arborization and axon guidance[56]. Variants that influence intracranial volume are clustered near genes involved in EGFR and phosphatidylinositol-3-OH kinase (PI(3)K)/AKT signalling pathways, known to be involved in neuronal survival[57]. All of these represent potential mechanisms by which genetic variants influence brain structure. It is important to note that the hybrid set-based test (HYST) method for pathway analysis used here can be strongly influenced by a few highly significant genes, as was the case for putamen hits in which *DCC* and *BCL2L1* were driving the pathway results.

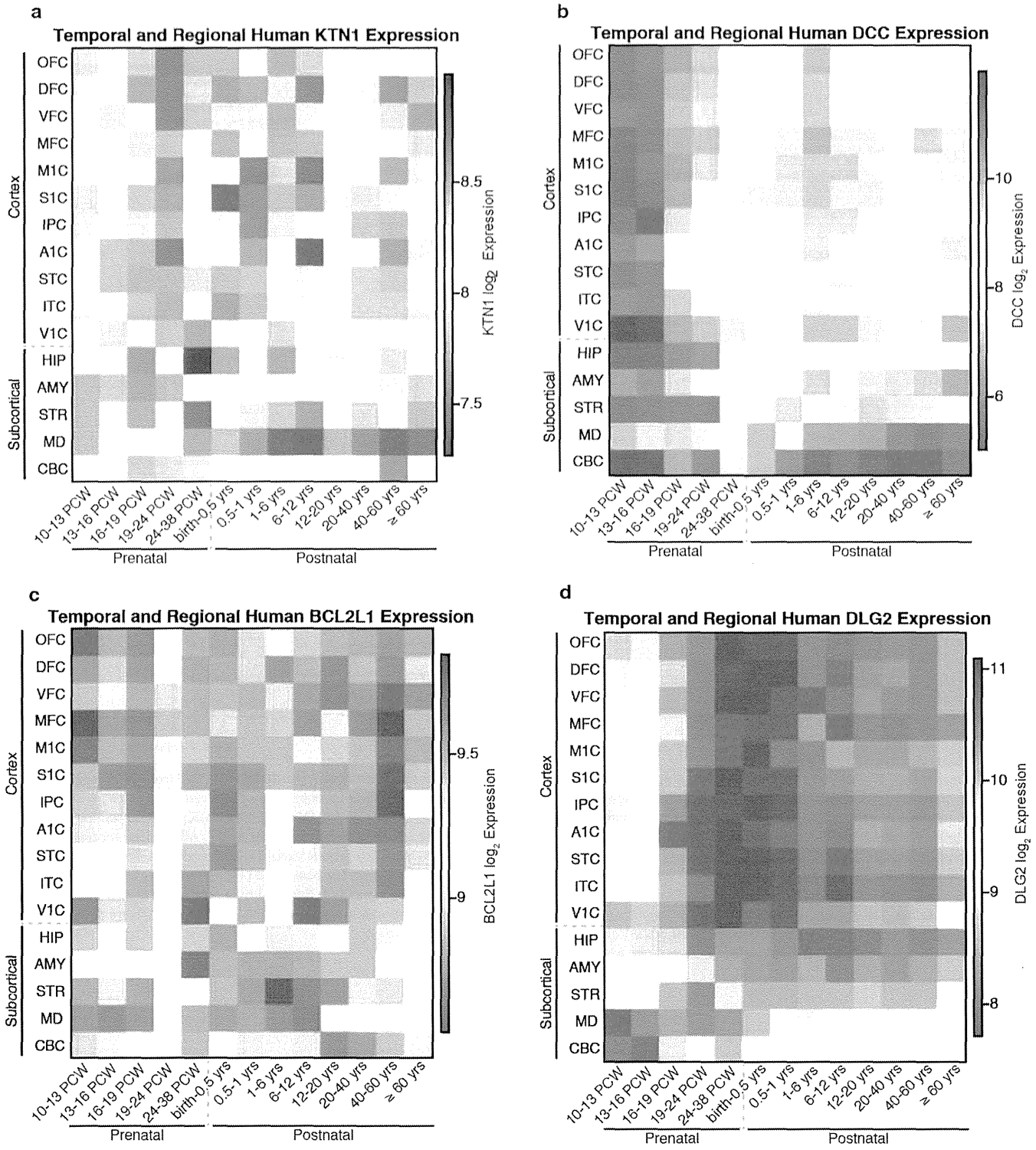

Extended Data Figure 8 | Spatio-temporal maps showing expression of genes near the four significant putamen loci over time and throughout regions of the brain. Spatio-temporal gene expression[13] was plotted as normalized $\log_2$ expression. Different areas of the neocortex (A1C, primary auditory cortex; DFC, dorsolateral prefrontal cortex; IPC, posterior inferior parietal cortex; ITC, inferior temporal cortex; MFC, medial prefrontal cortex; M1C, primary motor cortex; OFC, orbital prefrontal cortex; STC, superior temporal cortex; S1C, primary somatosensory cortex; VFC, ventrolateral prefrontal cortex; V1C, primary visual cortex) as well as subcortical areas (AMY, amygdala; CBC, cerebellar cortex; HIP, hippocampus; MD, mediodorsal nucleus of the thalamus; STR, striatum) are plotted from 10 post-conception weeks (PCW) to more than 60 years old. Genes that probably influence putamen volume are expressed in the striatum at some point during the lifespan. After late fetal development, *KTN1* is expressed in the human thalamus, striatum and hippocampus and is more highly expressed in the striatum than the cortex. Most genes seem to have strong gradients of expression across time, with *DCC* most highly expressed during early prenatal life, and *DLG2* most highly expressed at mid-fetal periods and throughout adulthood. *BCL2L1*, which inhibits programmed cell death, has decreased striatal expression at the end of neurogenesis (24–38 PCW), a period marked by increased apoptosis in the putamen[15].

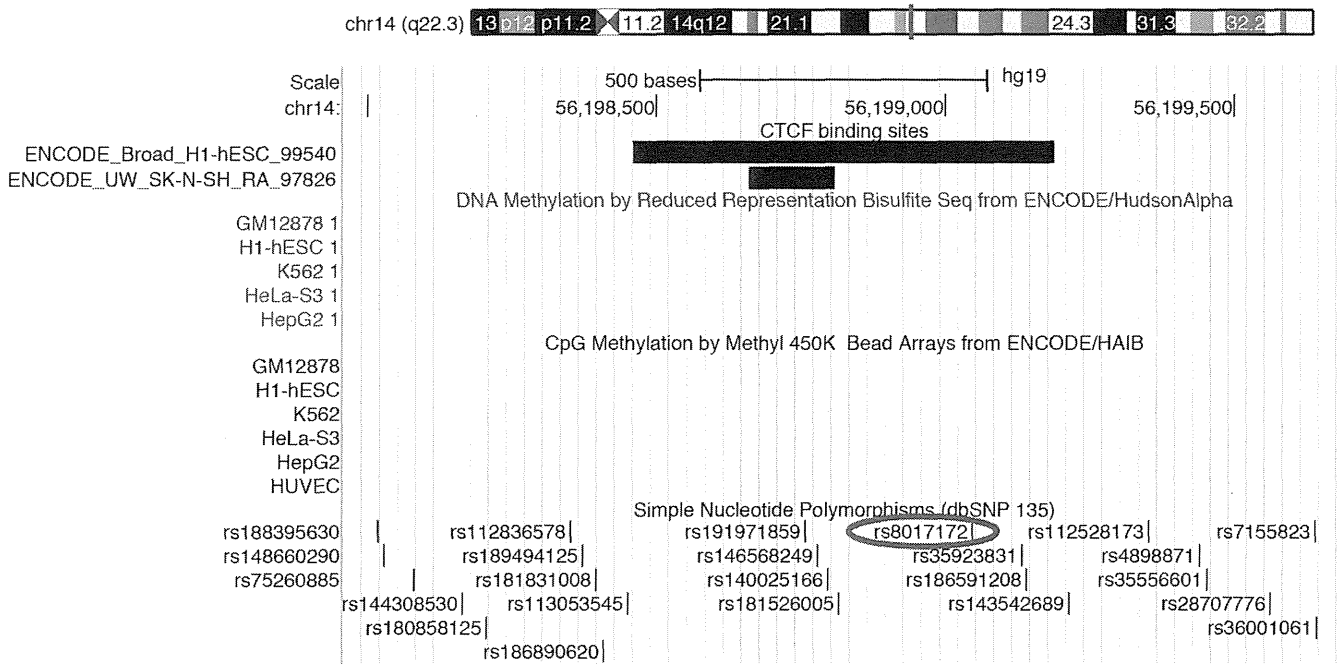

Extended Data Figure 9 | CTCF-binding sites in the vicinity of the putamen locus marked by rs945270. CTCF-binding sites from the ENCODE project are displayed from the database CTCFBSDB 2.0 (ref. 23) from two different cell types: embryonic stem cells (track ENCODE_Broad_H1-hESC_99540) and a neuroblastoma cell line differentiated with retinoic acid (ENCODE_UW_SK-N-SH_RA_97826). A proxy SNP to the top hit within the locus, rs8017172 (r^2 = 1.0 to rs945270), lies within a CTCF-binding site called based on ChIP-seq data in the embryonic stem cells and near the binding site in neural SK-N-SH cells. As this is the lone chromatin mark in the intergenic region (see Extended Data Fig. 3), it suggests that the variant may disrupt a CTCF-binding site and thereby influence transcription of surrounding genes.

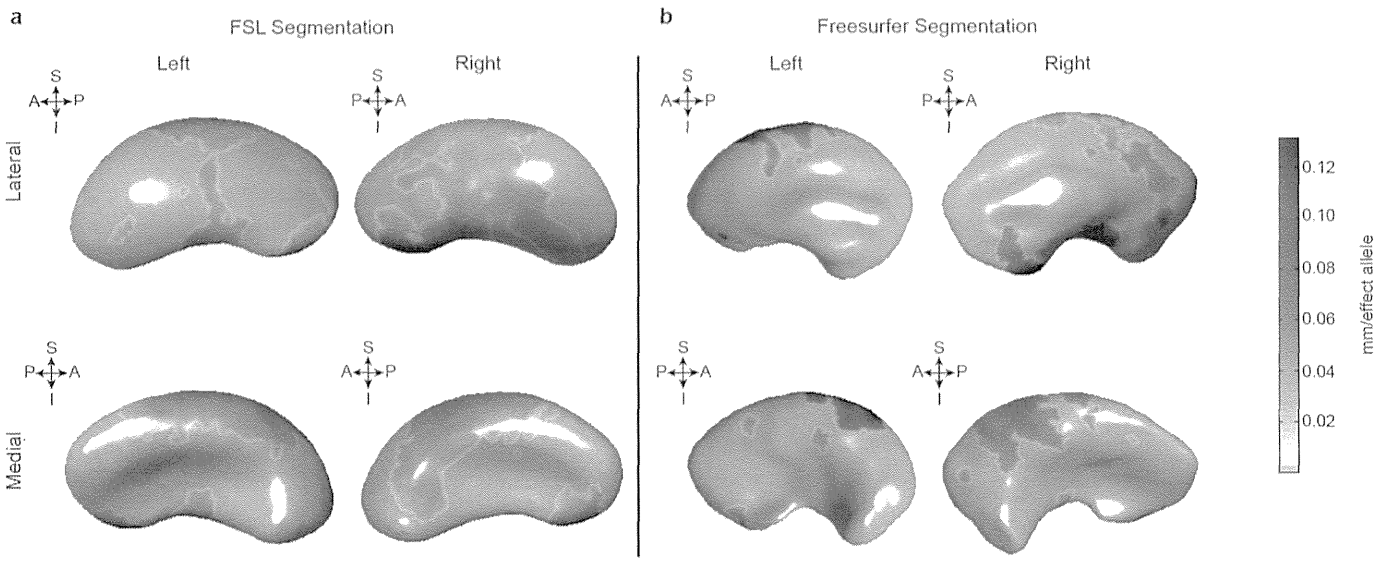

Extended Data Figure 10 | Shape analysis in 1,541 young healthy subjects shows consistent deformations of the putamen regardless of segmentation protocol. **a**, **b**, The distance from a medial core to surfaces derived from FSL FIRST (**a**; identical to Fig. 2c) or FreeSurfer (**b**) segmentations was derived in the same 1,541 subjects. Each copy of the *rs945270-C* allele was significantly associated with an increased width in coloured areas (false discovery rate corrected at $q = 0.05$) and the degree of deformation is labelled by colour. The orientation is indicated by arrows. A, anterior; I, inferior; P, posterior; S, superior. Shape analysis in both software suites gives statistically significant associations in the same direction. Although the effects are more widespread in the FSL segmentations, FreeSurfer segmentations also show overlapping regions of effect, which appears strongest in anterior and superior sections.

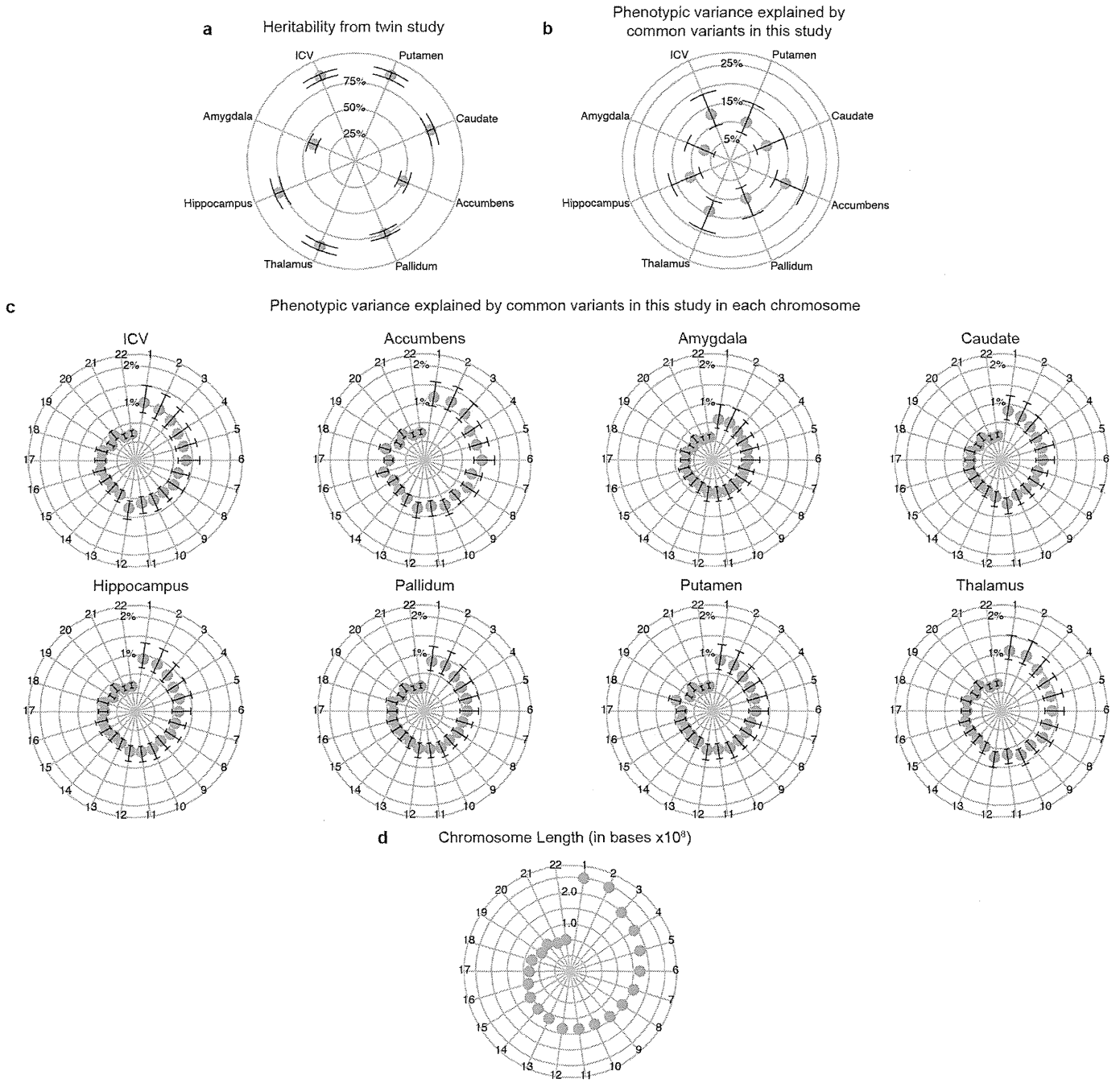

Extended Data Figure 11 | The phenotypic variance explained by all common variants in this study. **a**, Twin-based heritability (with 95% confidence intervals), measuring additive genetic influences from both common and rare variation, is shown for comparison with common variant based heritability (see Methods). **b**, The median estimated percentage of phenotypic variance explained by all SNPs (and 95% confidence interval) is given for each brain structure studied[41]. The full genome-wide association results from common variants explain approximately 7–15% of variance depending on the phenotype. **c**, The median estimated variance explained by each chromosome is shown for each phenotype. **d**, Some chromosomes explain more variance than would be expected by their length, for example chromosome 18 in the case of the putamen, which contains the *DCC* gene.

Schizophrenia Research 160 (2014) 228–229

Contents lists available at ScienceDirect

Schizophrenia Research

journal homepage: www.elsevier.com/locate/schres

Letter to the Editor

An integrated eye movement score as a neurophysiological marker of schizophrenia

Dear Editors

Patients with schizophrenia present with eye movement abnormalities. Some studies have shown that eye movement abnormalities were effective in distinguishing schizophrenia cases from healthy controls (Arolt et al., 1998; Campana et al., 1999; Benson et al., 2012), which suggests that eye movements could be a good biomarker of schizophrenia. Once an objectively defined quantity has been identified from eye movement characteristics, it will represent a beneficial clinical tool to assist in the diagnosis of schizophrenia and the estimation of the potential risk and genetic traits of schizophrenia.

In this study, we aimed to create an integrated eye movement rating scale that indicates the degree to which the eye movements are abnormal, and examined the relationship between the eye movement score and conventional scales of symptom severity and social and cognitive functioning in patients with schizophrenia. The eye movements of 40 patients with schizophrenia and 69 healthy subjects aged 15 to 68 years old were recorded (Supplementary material and methods and Table 1). All subjects were biologically unrelated and were of Japanese descent (Hashimoto et al., 2010; Ohi et al., 2013). The patients were recruited from the Osaka University Hospital and had been diagnosed by two or more trained psychiatrists according to the criteria from the Diagnostic and Statistical Manual of Mental Disorders, Fourth Edition (DSM-IV) based on the Structured Clinical Interview for DSM-IV (SCID). All participants provided written informed consent after the study procedures had been fully explained. This study was performed in accordance with the World Medical Association's Declaration of Helsinki and was approved by the Research Ethical Committee of Osaka University and the Kyoto University Graduate School and Faculty of Medicine, Ethics Committee. We administered examinations of smooth pursuit eye movements, steady fixations and exploratory eye movements described in Supplementary method in detail. We obtained 65 eye movement variables and carried out the discriminant analysis to create an integrated eye movement score that objectively represents normal to abnormal eye movements.

Significant differences between the patients with schizophrenia and the healthy subjects were observed in 27 variables (Supplementary Table 2). To create an integrative measure that effectively represents eye movement abnormality, a canonical discriminant analysis with a stepwise procedure was conducted using the 65 eye movement variables. Five of the 65 eye movement variables listed in Supplementary Table 3 were selected through this analysis. The created eye movement score was significantly different between patients with schizophrenia and controls ($U = 166$, $p = 2.3 \times 10^{-14}$) (Fig. 1). The correct rate of the discriminant analysis of these 5 variables was 89.9% in the resubstitution method and 88.1% in the leave-one out cross validation method (Supplementary Table 4), with a sensitivity and specificity of 0.78 and 0.94, respectively. This accuracy was comparable or even better than the classifications with electrophysiological endophenotypes (80%) (Price et al., 2006), a combination of the Wisconsin Card Sorting Test and Rorschach measures (89.4%) (Perry and Braff, 1998), a combination of the neuropsychological test battery and neurologic soft signs (81.8%) (Arango et al., 1999), or a combination of minor physiological anomalies and neurologic soft signs (82.9%) (John et al., 2008).

We examined the correlations between the eye movement score and the conventional symptom/functioning measures of schizophrenia in the patients and found marginal correlations with positive symptom ($r = -0.30$, $p = 0.06$), negative symptom ($r = -0.32$, $p = 0.04$), general psychopathology ($r = -0.31$, $p = 0.05$) in PANSS, the GAF ($r = 0.36$, $p = 0.02$) and the cognitive decline scores ($r = 0.34$, $p = 0.04$) (Supplementary Table 5). The integrated eye movement score represents the dimensions of schizophrenia that are, in large part, different from the dimensions represented by the conventional scales. Therefore, the score will effectively assist physicians' diagnosis together with conventional symptom/functioning scales, and, in particular, may be useful in the early diagnosis of schizophrenia or its prodrome where subjective symptoms are relatively obscure. The significance of eye movement scores primarily lies in diagnosis of schizophrenia, although this score is not to replace DSM-V diagnostic criteria or any

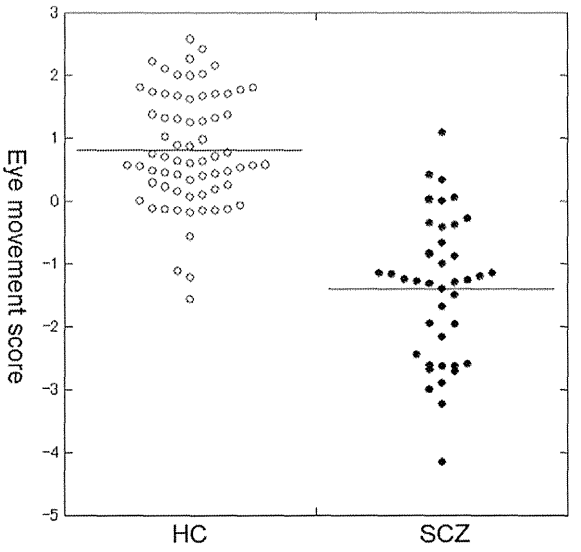

Fig. 1. Integrated eye movement score in patients with schizophrenia and controls. Integrated eye movement score (Y) in patients with schizophrenia (SCZ, $n = 40$) and healthy controls (HC, $n = 69$) was calculated by the following formula. $Y = 0.03 \times$ {Scanpath length (free viewing)} $+ 2.01 \times$ {V-Position gain (faster Lissajous)} $+ 0.03 \times$ {Fixation number (faster Lissajous)} $+ 0.37 \times$ {Fixation duration (far distracter)} $- 1.53 \times$ {S/N ratio (horizontal pursuit)} $- 4.92$. The bars represent mean values. $p = 2.3 \times 10^{-14}$, Mann Whitney U test.

http://dx.doi.org/10.1016/j.schres.2014.10.023

other criteria that rely on history, observation and self-report. A similar methodology using eye movement characteristics may be usable to distinguish schizophrenia from bipolar mania, schizoaffective disorder and autism and so on, and future studies should test this possibility.

Role of funding source

This work was supported, in part, by research grants from the Japanese Ministry of Health, Labour and Welfare (H22-seishin-ippan-001); the Japanese Ministry of Education, Culture, Sports, Science, and Technology (MEXT) KAKENHI [22390225-Grant-in-Aid for Scientific Research (B), 25293250-Grant-in-Aid for Scientific Research (B), 23659565-Grant-in-Aid for Challenging Exploratory Research and 221S0003-Grant-in-Aid for Scientific Research on Innovative Areas (Comprehensive Brain Science Network)]; and the Japan Foundation for Neuroscience and Mental Health, the Brain Sciences Project of the Center for Novel Science Initiatives (CNSI), the National Institutes of Natural Sciences (NINS) (grant number, BS251002).

Contributors

K. Miura was critically involved in the design, performed the analysis and interpretation of the data and wrote the manuscript. R. Hashimoto supervised the entire project, was critically involved in the design, analysis and interpretation of the data and was responsible for performing the literature review. M. Fujimoto, H. Yamamori, Y. Yasuda, K. Ohi, S. Umeda-Yano, M. Fukunaga, and M. Iwase were involved in the subject recruitment and the clinical diagnostic assessments and contributed intellectually to the data interpretation. M. Takeda supervised the study and contributed intellectually to the data interpretation. All authors contributed to and have approved the final manuscript.

Conflict of interest

All authors declare that they have no conflicts of interest.

Acknowledgments

We would like to thank the subjects who participated in this study.

Appendix A. Supplementary data

Supplementary data to this article can be found online at http://dx.doi.org/10.1016/j.schres.2014.10.023.

References

Arango, C., Bartko, J.J., Gold, J.M., Buchanan, R.W., 1999. Prediction of neuropsychological performance by neurological signs in schizophrenia. Am. J. Psychiatry 156 (9), 1349–1357.

Arolt, V., Teichert, H.M., Steege, D., Lencer, R., Heide, W., 1998. Distinguishing schizophrenic patients from healthy controls by quantitative measurement of eye movement parameters. Biol. Psychiatry 44 (6), 448–458.

Benson, P.J., Beedie, S.A., Shephard, E., Giegling, I., Rujescu, D., St Clair, D., 2012. Simple viewing tests can detect eye movement abnormalities that distinguish schizophrenia cases from controls with exceptional accuracy. Biol. Psychiatry 72 (9), 716–724.

Campana, A., Duci, A., Gambini, O., Scarone, S., 1999. An artificial neural network that uses eye-tracking performance to identify patients with schizophrenia. Schizophr. Bull. 25 (4), 789–799.

Hashimoto, R., Ohi, K., Yasuda, Y., Fukumoto, M., Iwase, M., Iike, N., Azechi, M., Ikezawa, K., Takaya, M., Takahashi, H., Yamamori, H., Okochi, T., Tanimukai, H., Tagami, S., Morihara, T., Okochi, M., Tanaka, T., Kudo, T., Kazui, H., Iwata, N., Takeda, M., 2010. The impact of a genome-wide supported psychosis variant in the ZNF804A gene on memory function in schizophrenia. Am. J. Med. Genet. B Neuropsychiatr. Genet. 153B (8), 1459–1464.

John, J.P., Arunachalam, V., Ratnam, B., Isaac, M.K., 2008. Expanding the schizophrenia phenotype: a composite evaluation of neurodevelopmental markers. Compr. Psychiatry 49 (1), 78–86.

Ohi, K., Hashimoto, R., Yamamori, H., Yasuda, Y., Fujimoto, M., Umeda-Yano, S., Fukunaga, M., Watanabe, Y., Iwase, M., Kazui, H., Takeda, M., 2013. The impact of the genome-wide supported variant in the cyclin M2 gene on gray matter morphology in schizophrenia. Behav. Brain Funct. 9, 40.

Perry, W., Braff, D.L., 1998. A multimethod approach to assessing perseverations in schizophrenia patients. Schizophr. Res. 33 (1–2), 69–77.

Price, G.W., Michie, P.T., Johnston, J., Innes-Brown, H., Kent, A., Clissa, P., Jablensky, A.V., 2006. A multivariate electrophysiological endophenotype, from a unitary cohort, shows greater research utility than any single feature in the Western Australian family study of schizophrenia. Biol. Psychiatry 60 (1), 1–10.

Kenichiro Miura
Department of Integrative Brain Science, Graduate School of Medicine, Kyoto University, Japan
Correspondence to: K. Miura, Department of Integrative Brain Science, Graduate School of Medicine, Kyoto University, Konoe-cho, Yoshida, Kyoto-shi, Kyoto 606-8501, Japan. Tel.: +81 75 753 4481; fax: +81 75 753 4486.
E-mail address: kmiura@brain.med.kyoto-u.ac.jp.

Ryota Hashimoto
Department of Psychiatry, Osaka University Graduate School of Medicine, Osaka, Japan
Molecular Research Center for Children's Mental Development, United Graduate School of Child Development, Osaka University, Osaka, Japan
Correspondence to: R. Hashimoto, Molecular Research Center for Children's Mental Development, United Graduate School of Child Development, Osaka University, D3, 2-2, Yamadaoka, Suita, Osaka 5650871, Japan. Tel./fax: +81 6 6879 3074.
E-mail address: hashimor@psy.med.osaka-u.ac.jp.

Michiko Fujimoto
Department of Psychiatry, Osaka University Graduate School of Medicine, Osaka, Japan

Hidenaga Yamamori
Department of Psychiatry, Osaka University Graduate School of Medicine, Osaka, Japan
Department of Molecular Neuropsychiatry, Osaka University Graduate School of Medicine, Osaka, Japan

Yuka Yasuda
Department of Psychiatry, Osaka University Graduate School of Medicine, Osaka, Japan

Kazutaka Ohi
Department of Psychiatry, Osaka University Graduate School of Medicine, Osaka, Japan

Satomi Umeda-Yano
Department of Molecular Neuropsychiatry, Osaka University Graduate School of Medicine, Osaka, Japan

Masaki Fukunaga
Division of Cerebral Integration, National Institute for Physiological Sciences, Okazaki, Aichi, Japan

Masao Iwase
Department of Psychiatry, Osaka University Graduate School of Medicine, Osaka, Japan

Masatoshi Takeda
Department of Psychiatry, Osaka University Graduate School of Medicine, Osaka, Japan
Molecular Research Center for Children's Mental Development, United Graduate School of Child Development, Osaka University, Osaka, Japan

2 July 2014

Neurobiology of Aging 35 (2014) 2883.e1–2883.e2

Contents lists available at ScienceDirect

Neurobiology of Aging

journal homepage: www.elsevier.com/locate/neuaging

Negative results

Failure of replicating the association between hippocampal volume and 3 single-nucleotide polymorphisms identified from the European genome-wide association study in Asian populations

Ming Li [a,b,1], Kazutaka Ohi [b,c,1], Chunhui Chen [d,1], Qinghua He [d], Jie-wei Liu [a], Chuansheng Chen [e], Xiong-jian Luo [f], Qi Dong [d,**], Ryota Hashimoto [c,g,***], Bing Su [a,*]

[a] State Key Laboratory of Genetic Resources and Evolution, Kunming Institute of Zoology, Chinese Academy of Sciences, Kunming, Yunnan, China
[b] Lieber Institute for Brain Development, Johns Hopkins University, Baltimore, MD, USA
[c] Department of Psychiatry, Osaka University Graduate School of Medicine, Suita, Osaka, Japan
[d] State Key Laboratory of Cognitive Neuroscience and Learning, Beijing Normal University, Beijing, China
[e] Department of Psychology and Social Behavior, University of California, Irvine, CA, USA
[f] Key Laboratory of Animal Models and Human Disease Mechanisms of the Chinese Academy of Sciences & Yunnan Province, Kunming Institute of Zoology, Chinese Academy of Sciences, Kunming, Yunnan, China
[g] Molecular Research Center for Children's Mental Development, United Graduate School of Child Development, Osaka University, Suita, Osaka, Japan

ARTICLE INFO

Article history:
Received 30 August 2013
Received in revised form 9 July 2014
Accepted 12 July 2014
Available online 19 July 2014

Keywords:
Hippocampal volume
GWAS
Replication study
Asian

ABSTRACT

Hippocampal volume is a key brain structure for learning ability and memory process, and hippocampal atrophy is a recognized biological marker of Alzheimer's disease. However, the genetic bases of hippocampal volume are still unclear although it is a heritable trait. Genome-wide association studies (GWASs) on hippocampal volume have implicated several significantly associated genetic variants in Europeans. Here, to test the contributions of these GWASs identified genetic variants to hippocampal volume in different ethnic populations, we screened the GWAS-identified candidate single-nucleotide polymorphisms in 3 independent healthy Asian brain imaging samples (a total of 990 subjects). The results showed that none of these single-nucleotide polymorphisms were associated with hippocampal volume in either individual or combined Asian samples. The replication results suggested a complexity of genetic architecture for hippocampal volume and potential genetic heterogeneity between different ethnic populations.

1. Introduction

Hippocampal volume, a heritable trait associated with cognition in humans, is considered to be a suitable endophenotype for aging-related physiological processes and presymptomatic diseases, such as Alzheimer's disease. However, the genetic basis of hippocampal volume is still unclear.

Recently, the Cohorts for Heart and Aging Research in Genomic Epidemiology and the Enhancing Neuro Imaging Genetics through Meta-Analysis consortia have performed independent genome-wide association studies on hippocampal volume in different samples of European ancestry, and they identified 5 significantly associated genetic variants (rs17178006, rs6581612, rs6741949, rs7852872, and rs7294919) (Bis et al., 2012; Stein et al., 2012). Because the analyses were mostly conducted in Europeans, and the associations in other populations are yet to be tested.

2. Methods

We recruited a total of 990 healthy Asian subjects from 3 locations: 294 Chinese individuals from Kunming in southwestern China, 331 Chinese individuals from Beijing in northern China, and 365 Japanese subjects from Osaka, Japan. Among the 5 candidate

* Corresponding author at: State Key Laboratory of Genetic Resources and Evolution, Kunming Institute of Zoology, Chinese Academy of Sciences, 32 East Jiaochang Road, Kunming 650223, Yunnan, China. Tel.: +86 871 5120212; fax: +86 871 65193137.
** Co-Corresponding author at: State Key Laboratory of Cognitive Neuroscience and Learning, Beijing Normal University, Beijing 100875, China. fax: +86-010-58808470.
*** Co-Corresponding author at: Department of Psychiatry, Osaka University Graduate School of Medicine, Osaka, Japan.
E-mail addresses: dongqi@bnu.edu.cn (Q. Dong), hashimor@psy.med.osaka-u.ac.jp (R. Hashimoto), sub@mail.kiz.ac.cn (B. Su).
[1] These authors contributed equally to this work.

0197-4580/$ – see front matter © 2014 Elsevier Inc. All rights reserved.
http://dx.doi.org/10.1016/j.neurobiolaging.2014.07.015

Table 1
Replications of GWAS-identified SNPs on mean bilateral hippocampal volume in Asian populations

Locus	SNP	Populations	Sample size	Effect allele	Frequency	β (mm^3)	SE (mm^3)	*p*-value
2q24.3	rs6741949	Chinese (Kunming)	288	G	0.903	35.85	57.27	0.53
		Chinese (Beijing)	331	G	0.929	16.97	55.99	0.76
		Japanese (Osaka)	363	G	0.934	−49.30	41.82	0.24
		Combined Asians	**982**	**G**	**0.923**	**−9.91**	**28.92**	**0.73**
9q33.1	rs7852872	Chinese (Kunming)	288	C	0.427	34.37	31.90	0.28
		Japanese (Osaka)	361	C	0.431	−6.76	21.21	0.75
		Combined Asians	**649**	**C**	**0.429**	**5.85**	**17.66**	**0.74**
12q24.22	rs7294919	Chinese (Kunming)	288	C	0.161	−32.40	46.02	0.48
		Chinese (Beijing)	331	C	0.239	−1.98	35.19	0.96
		Japanese (Osaka)	365	C	0.203	−24.33	26.05	0.35
		Combined Asians	**984**	**C**	**0.203**	**−19.16**	**19.06**	**0.31**

Frequency, the frequency of the effect allele. β represents the difference in hippocampal volumes per copy increase of effect allele. Sex, age, age^2, sex × age, sex × age^2, and total intracranial volume (ICV) were included as covariates.
The combined sample and their results were marked in bold.
Key: GWAS, genome-wide association study; SE, standard error; SNPs, single-nucleotide polymorphisms.

single-nucleotide polymorphisms (SNPs) from genome-wide association studies, 2 of them (rs17178006 and rs6581612) are monomorphic in Asians according to the data from the 1000-Human-Genome (1000 Genomes Project Consortium et al., 2012); therefore, only the other 3 SNPs (rs6741949, rs7852872, and rs7294919) were included for further analysis. The effects of the 3 SNPs on mean bilateral hippocampal volume (as well as left and right hippocampal volume, separately) were analyzed using linear regression with sex, age, age^2, sex × age, sex × age^2, intracranial volume, and multidimensional scaling components (optional) as covariates, and dummy variables for different scanners or acquisition sequences were also included as covariates when analyzing the combined samples. Details about sample information, structural magnetic resonance imaging acquisition, image preprocessing, and statistical analyses were shown in Supplementary Material and Supplementary Table 1.

3. Results

Our primary replication results were shown in Table 1. None of the candidate SNPs were associated with mean bilateral hippocampal volumes in either individual sample or combined samples. We also assessed the associations by altering covariates (such as removing intracranial volume or including multidimensional scaling components), and the results remained nonsignificant (Supplementary Tables 2 and 3). The associations for left or right hippocampal volume were both not significant (Supplementary Tables 4 and 5). In addition, these SNPs were not associated with intracranial volume (Supplementary Table 6) or other factors (e.g., sex, age and so forth) either, excluding the possibility of the negative results caused by these factors.

We performed power analysis based on our sample size (a total of 990 subjects) using the genetic power calculator, and the analyses showed that we had over 80.0% power to detect risk variants with effect size of 2% of the variance, suggesting that our results are reliable.

4. Discussion

Our results did not show evidence of associations for the SNPs in our Asian samples. We performed the power calculation on our sample size and it is of enough power to identify true variants showing nominal significant associations ($p < 0.05$). Effect size (β) is a measure of the strength of a phenomenon such as hippocampal volume variation; if an SNP contributes to hippocampal volume variation equally in different populations, the effect size should be the same between samples, but the *p*-value and standard error will vary because of differences in sample size; therefore, we also compared the effect sizes (β) of the SNPs between our Asian samples and Europeans. We found the effect sizes (β) in Asians were closer to zero compared with the results in Europeans (−9.91 mm^3 vs. −52.80 mm^3 for rs6741949-G; 5.85 mm^3 vs. −47.70 mm^3 for rs7852872-C; −19.16 mm^3 vs. 47.58 mm^3 for rs7294919-C), and the directions of β varied among the Asian samples (Table 1), indicating these SNPs unlikely contribute to large effects to hippocampal volume variation in Asians.

Notably, the genetic bases of hippocampal volume are very complex, likely with many involved variants of small effects. Although our imaging samples have been shown to be effective for the detection of genetic effects on hippocampal volumes extracted from the magnetic resonance imaging data (Li et al., 2013; Zhu et al., 2013), we are still unable to detect extremely weak effect variants. More importantly, the most likely reason for the failure of replication is the well-known genetic divergences between European and Asian populations, which are common in genetic analyses of complex traits and disorders in world populations.

Disclosure statement

The authors have no conflicts of interest to disclose.

Acknowledgements

This work was supported by grants from the National 973 project of China (2011CBA00401), the National Natural Science Foundation of China (U1202225), and the 111 Project (B07008) of the Ministry of Education of China, the Japanese Ministry of Education, Culture, Sports, Science and Technology (18689030, 22390225).

Appendix A. Supplementary data

Supplementary data associated with this article can be found, in the online version, at http://dx.doi.org/10.1016/j.neurobiolaging.2014.07.015.

OPEN

Citation: Transl Psychiatry (2014) **4**, e472; doi:10.1038/tp.2014.110

www.nature.com/tp

ORIGINAL ARTICLE

Common variants at 1p36 are associated with superior frontal gyrus volume

R Hashimoto[1,2,13], M Ikeda[3,13], F Yamashita[4], K Ohi[2], H Yamamori[2,5], Y Yasuda[2], M Fujimoto[2], M Fukunaga[6], K Nemoto[7], T Takahashi[8], M Tochigi[9], T Onitsuka[10], H Yamasue[9], K Matsuo[11], T Iidaka[12], N Iwata[3], M Suzuki[8], M Takeda[1,2], K Kasai[9] and N Ozaki[12]

The superior frontal gyrus (SFG), an area of the brain frequently found to have reduced gray matter in patients with schizophrenia, is involved in self-awareness and emotion, which are impaired in schizophrenia. However, no genome-wide association studies of SFG volume have investigated in patients with schizophrenia. To identify single-nucleotide polymorphisms (SNPs) associated with SFG volumes, we demonstrated a genome-wide association study (GWAS) of gray matter volumes in the right or left SFG of 158 patients with schizophrenia and 378 healthy subjects. We attempted to bioinformatically ascertain the potential effects of the top hit polymorphism on the expression levels of genes at the genome-wide region. We found associations between five variants on 1p36.12 and the right SFG volume at a widely used benchmark for genome-wide significance ($P < 5.0 \times 10^{-8}$). The strongest association was observed at rs4654899, an intronic SNP in the eukaryotic translation initiation factor 4 gamma, 3 (*EIF4G3*) gene on 1p36.12 ($P = 7.5 \times 10^{-9}$). No SNP with genome-wide significance was found in the volume of the left SFG ($P > 5.0 \times 10^{-8}$); however, the rs4654899 polymorphism was identified as the locus with the second strongest association with the volume of the left SFG ($P = 1.5 \times 10^{-6}$). *In silico* analyses revealed a proxy SNP of rs4654899 had effect on gene expression of two genes, *HP1BP3* lying 3′ to *EIF4G3* ($P = 7.8 \times 10^{-6}$) and *CAPN14* at 2p ($P = 6.3 \times 10^{-6}$), which are expressed in moderate-to-high levels throughout the adult human SFG. These results contribute to understand genetic architecture of a brain structure possibly linked to the pathophysiology of schizophrenia.

Translational Psychiatry (2014) **4,** e472; doi:10.1038/tp.2014.110; published online 21 October 2014

INTRODUCTION

Schizophrenia is a common and complex psychiatric disorder with a lifetime risk of approximately 1%. This disorder has a strong genetic component; the estimated heritability is 81%.[1] Multiple genetic variants that have a small effect have been implicated in the pathogenesis of schizophrenia.[2] A genome-wide association study (GWAS) of single-nucleotide polymorphisms (SNPs) that accesses tens of thousands of DNA samples from patients and controls can be a powerful tool for identifying common risk factors for complex diseases, such as schizophrenia. GWASs on schizophrenia have identified several genome-wide significant associated variants.[3,4] Subsequently, GWASs on neurobiological quantitative traits as intermediate phenotypes that possibly reflect the underlying genetic vulnerability better than diagnostic categorization, such as schizophrenia,[5,6] have been performed to minimize the clinical and genetic heterogeneity in studies of schizophrenia.[7]

The superior frontal gyrus (SFG) of the brain is frequently found to have reduced gray matter in individuals with first-episode schizophrenia and neuroleptic naive schizophrenia, as well as chronic patients with schizophrenia.[8,9] The SFG is involved in self-awareness and emotion.[10,11] Self-awareness is the cognitive ability to differentiate between self and non-self cues and is necessary to understand the behavior of other humans. Disturbance in self-awareness linked to social cognition is a core feature of schizophrenia.[12] Emotional disturbances, including meaningless laughter, are often observed in patients with schizophrenia. Meaningless laughter was also observed in unaffected siblings of schizophrenia, thus indicating its heritability.[13] In addition, laughter can be elicited by electrical stimulation of the SFG. Gray matter volumes of bilateral SFG have a strong genetic component, with an estimated heritability of 76–80%.[14] As there is considerable inter-individual variation in the degree of reduced volume of the SFG, it appears that genetic influences have a role in determining the degree of volume reduction of the SFG in schizophrenia. Although GWASs of bilateral hippocampal volume have recently been reported,[15,16] no study has investigated other brain areas in patients with schizophrenia. To identify an SNP related to SFG volumes, we conducted a GWAS of gray matter volumes in the right or left SFG of patients with schizophrenia and healthy subjects.

[1]Molecular Research Center for Children's Mental Development, United Graduate School of Child Development, Osaka University, Suita, Osaka, Japan; [2]Department of Psychiatry, Osaka University Graduate School of Medicine, Suita, Osaka, Japan; [3]Department of Psychiatry, Fujita Health University School of Medicine, Toyoake, Aichi, Japan; [4]Division of Ultrahigh Field MRI, Institute for Biomedical Sciences, Iwate Medical University, Yahaba, Iwate, Japan; [5]Department of Molecular Neuropsychiatry, Osaka University Graduate School of Medicine, Suita, Osaka, Japan; [6]Biofunctional Imaging, Immunology Frontier Research Center, Osaka University, Suita, Osaka, Japan; [7]Department of Neuropsychiatry, Institute of Clinical Medicine, University of Tsukuba, Ibaraki, Japan; [8]Department of Neuropsychiatry, Graduate School of Medicine and Pharmaceutical Sciences, University of Toyama, Toyama, Japan; [9]Department of Neuropsychiatry, Graduate School of Medicine, University of Tokyo, Tokyo, Japan; [10]Department of Neuropsychiatry, Graduate School of Medical Sciences, Kyushu University, Fukuoka, Japan; [11]Division of Neuropsychiatry, Department of Neuroscience, Yamaguchi University Graduate School of Medicine, Yamaguchi, Japan and [12]Department of Psychiatry, Nagoya University Graduate School of Medicine, Nagoya, Aichi, Japan. Correspondence: Professor R Hashimoto, Molecular Research Center for Children's Mental Development, United Graduate School of Child Development, Osaka University, D3, 2-2, Yamadaoka, Suita, Osaka 5650871, Japan.
E-mail: hashimor@psy.med.osaka-u.ac.jp
[13]These authors contributed equally to this work.
Received 3 June 2014; revised 4 August 2014; accepted 31 August 2014

MATERIALS AND METHODS

Subjects

We selected 281 patients with schizophrenia (52.0% males, 146 males and 135 females; mean age 36.0 ± 12.4 years) and 413 healthy controls (49.6% males, 205 males and 208 females; mean age 36.4 ± 12.8 years) for a GWAS of schizophrenia-related phenotypes, such as structural brain morphology, neurocognitive function and neurophysiological assessments.[17–19] All of the subjects were biologically unrelated, there were no first- or second-degree relatives, and all were of Japanese descent.[20,21] The subjects were excluded if they had neurological or medical conditions that could potentially affect the central nervous system, such as atypical headaches, head trauma with loss of consciousness, chronic lung disease, kidney disease, chronic hepatic disease, thyroid disease, active cancer, cerebrovascular disease, epilepsy, seizures, substance-related disorders or mental retardation. Patients with schizophrenia were recruited from the Osaka University Hospital. Each patient had been diagnosed by at least two trained psychiatrists according to the criteria from the DSM-IV (Diagnostic and Statistical Manual of Mental Disorders, Fourth Edition) based on the Structured Clinical Interview for DSM-IV. Current symptoms of schizophrenia were evaluated using the positive and negative syndrome scale. Controls were recruited through local advertisements at Osaka University. The healthy subjects were evaluated using the non-patient version of the Structured Clinical Interview for DSM-IV to exclude individuals who had current or past contact with psychiatric services or who had received psychiatric medications.

Superior frontal volumes obtained from the magnetic resonance imaging data were assessed in 158 patients with schizophrenia and 378 healthy subjects. Detailed demographic information is shown in Supplementary Table S1. Mean age and handedness did not differ significantly between the cases and controls ($P > 0.50$); however, the gender ratio, years of education and estimated premorbid intelligence quotient differed significantly between the cases and controls ($P < 0.05$). The ratio of male was higher in patients with schizophrenia compared with the controls. The years of education and estimated premorbid intelligence quotient were significantly lower in patients with schizophrenia compared with the controls. When the genotype groups in the top five SNPs with genome-wide significance of the right SFG volume were compared within the patient and control groups, we found no differences across the demographic variables, except for the gender ratio in the controls (rs6700718, rs1354792, rs10218584, and rs6702110; $P < 0.05$). Written informed consent was obtained from all the subjects after the procedures had been fully explained. This study was performed in accordance with the World Medical Association's Declaration of Helsinki and was approved by the Research Ethical Committee of Osaka University.

Magnetic resonance imaging procedure and extraction of SFG volumes

All magnetic resonance imaging data were obtained using a 1.5-T GE Signa EXCITE system (Tokyo, Japan). A three-dimensional volumetric acquisition of a T1-weighted gradient echo sequence produced a gapless series of 124 sagittal sections using a spoiled gradient-recalled acquisition in the steady state (SPGR) sequence (TE/TR, 4.2/12.6 ms; flip angle, 15°; acquisition matrix, 256 × 256; 1NEX, FOV, 24 × 24 cm; slice thickness, 1.4 mm). We screened all scans and found no gross abnormalities, such as infarcts, hemorrhages or brain tumors, in any of the subjects. Each image was visually examined to eliminate any images with motion or metal artifacts, and the anterior commissure–posterior commissure line was adjusted.[22] MR images were processed with the VBM8 toolbox (http://dbm.neuro.uni-jena.de/vbm/download/) implemented for SPM8 (Wellcome Department of Imaging Neuroscience, University College London, UK, http://www.fil.ion.ucl.ac.uk/spm) running in MATLAB (The Mathworks, Natick, MA, USA) for tissue segmentation and anatomical normalization, as described elsewhere.[23–25] The voxel values of the normalized gray matter images were modulated according to the nonlinear component of the transformation, which resulted in approximating brain-size-adjusted gray matter volumes while preserving local volume changes.[26] Gray matter volumes of the bilateral SFG were then calculated by using the maximum probabilistic atlas using 20 hand-labeled images (Supplementary Figure S1).[27,28]

SNP selection and SNP genotyping

Genotyping was performed using the Affymetrix Genome-Wide Human SNP Array 6.0 (Affymetrix, Santa Clara, CA, USA), according to the manufacturer's protocol. The genotypes were called from the CEL files using Birdseed v2 for the 6.0 chip implemented in the Genotyping Console software (Affymetrix). We then applied the following quality control (QC) criteria to exclude samples: (i) arrays with low QC (< 0.4) according to Birdseed v2 ($N = 0$), (ii) samples for which < 95% of the genotypes were called ($N = 0$) and (iii) samples in the same family according to $\hat{\pi}$ (> 0.4, $N = 0$). Next, we excluded SNPs that: (i) had low call rates (< 0.95), (ii) were duplicated, (iii) were localized to sex chromosomes, (iv) deviated from Hardy–Weinberg equilibrium in the controls ($P < 0.0001$) or (v) had low minor allele frequencies < 0.05. After all of these exclusions, 517 946 SNPs that underwent QC remained for experimental analysis.

To test for the existence of a genetic structure in the data, we performed a principal component analysis using EIGENSTRAT 3.0 software.[29] Ten eigenvectors were calculated. Genotype information from the JPT (Japanese in Tokyo, Japan), CHB (Han Chinese in Beijing, China), CEU (Utah residents with ancestors from northern and western Europe) and YRI (Yoruba in Ibadan, Nigeria) in HapMap phase III was compared with our data set to check for population stratification (Supplementary Figure S2).

Statistical analyses

Statistical analyses of the demographic variables were performed using PASW Statistics 18.0 software (SPSS Japan, Tokyo, Japan). Differences in the clinical characteristics between patients and controls were analyzed using χ^2 tests for the categorical variables and the Mann–Whitney *U*-test for the continuous variables. Multiple linear regression analysis was performed to compare the gray matter volumes in the right and left SFG regions among genotypes (the number of major alleles; 0, 1 or 2) using PLINK 1.07 software. Diagnosis, age and gender were included as covariates. Quantile–Quantile is listed in Supplementary Figure S3.

RESULTS

We observed associations between five variants (rs4654899, rs6702110, rs6700718, rs10218584 and rs1354792) on 1p36.12 and the right SFG volume at a widely used benchmark for genome-wide significance ($P < 5.0 \times 10^{-8}$, r^2 among SNPs > 0.8; Figure 1). The strongest association was observed at rs4654899, an intronic SNP in the eukaryotic translation initiation factor 4 gamma, 3 (*EIF4G3*) gene on 1p36.12 ($P = 7.5 \times 10^{-9}$; Figure 2). No SNP with genome-wide significance was found in the volume of the left SFG; however, the rs4654899 polymorphism was identified as the locus with the second strongest association with the volume of the left SFG ($P = 1.5 \times 10^{-6}$; Figure 1). The top 10 and top 200 markers on each SFG are shown in Tables 1 and 2 and Supplementary Tables S2 and S3. *Post hoc* analyses separately assessed in patients and controls also revealed reduced but significant associations (Tables 1 and 2 and Supplementary Tables S2 and S3). Genotype effects of rs4654899 on gray matter volume of right superior frontal gyrus were found in patients with schizophrenia and controls (Figure 3). We attempted to bioinformatically ascertain the potential effects of the rs4654899 polymorphism on the expression levels of genes at the genome-wide region by using the mRNA by SNP Browser 1.0.1 database (http://www.sph.umich.edu/csg/liang/asthma/). Significant effects of the rs3767248 proxy SNP for rs4654899 ($r^2 = 1.0$) were identified

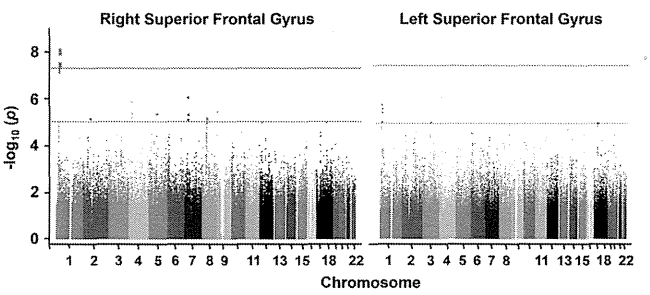

Figure 1. Manhattan plots derived from the multiple linear regression analysis of the bilateral superior frontal volumes. The blue line indicates a *P*-value of 1.0E−05. The red line indicates a *P*-value of 5.0E−08.